AGU PUBLICATIONS

Geophysical Research Letters

RESEARCH LETTER
10.1002/2016GL069163

Key Points:
- Energetic electrons at Mercury map magnetic topology at ~150 ms
- First direct observation of flux transfer event open-field topology at Mercury
- Modulations of the reconnection rate at Mercury occur at ion kinetic scales

Correspondence to:
D. J. Gershman,
daniel.j.gershman@nasa.gov

Citation:
Gershman, D. J., J. C. Dorelli, G. A. DiBraccio, J. M. Raines, J. A. Slavin, G. Poh, and T. H. Zurbuchen (2016), Ion-scale structure in Mercury's magnetopause reconnection diffusion region, *Geophys. Res. Lett.*, *43*, 5935–5942, doi:10.1002/2016GL069163.

Received 14 APR 2016
Accepted 11 MAY 2016
Accepted article online 14 MAY 2016
Published online 20 JUN 2016

Ion-scale structure in Mercury's magnetopause reconnection diffusion region

Daniel J. Gershman[1,2], John C. Dorelli[2], Gina A. DiBraccio[2], Jim M. Raines[3], James A. Slavin[3], Gangkai Poh[3], and Thomas H. Zurbuchen[3]

[1]Department of Astronomy, University of Maryland, College Park, Maryland, USA, [2]NASA Goddard Space Flight Center, Greenbelt, Maryland, USA, [3]Climate and Space Sciences and Engineering, University of Michigan, Ann Arbor, Michigan, USA

Abstract The strength and time dependence of the electric field in a magnetopause diffusion region relate to the rate of magnetic reconnection between the solar wind and a planetary magnetic field. Here we use ~150 ms measurements of energetic electrons from the Mercury Surface, Space Environment, GEochemistry, and Ranging (MESSENGER) spacecraft observed over Mercury's dayside polar cap boundary (PCB) to infer such small-scale changes in magnetic topology and reconnection rates. We provide the first direct measurement of open magnetic topology in flux transfer events at Mercury, structures thought to account for a significant portion of the open magnetic flux transport throughout the magnetosphere. In addition, variations in PCB latitude likely correspond to intermittent bursts of ~0.3–3 mV/m reconnection electric fields separated by ~5–10 s, resulting in average and peak normalized dayside reconnection rates of ~0.02 and ~0.2, respectively. These data demonstrate that structure in the magnetopause diffusion region at Mercury occurs at the smallest ion scales relevant to reconnection physics.

1. Introduction

Magnetic reconnection is a ubiquitous process in space plasmas whereby magnetic topology is reconfigured and magnetic energy is converted into particle energy. The important physical processes relevant to this conversion take place within a diffusion region, where ion and electron motions decouple from both each other and from the background magnetic field, and where the "frozen-in-field" approximation in space plasmas is no longer valid [*Parker*, 1957; *Sweet*, 1958]. In a planetary magnetosphere, magnetic reconnection can occur at the dayside magnetopause, where the interplanetary magnetic field (IMF) carried by the solar wind interacts with that of a planetary body. Here the closed magnetic flux (i.e., connected to the planetary body only) is converted into open flux (i.e., connected to the planetary body and the solar wind).

The topological boundary between the last closed field line and first open field line in the magnetosphere maps the magnetopause diffusion region to the polar cap boundary (PCB), which encloses all the planetary open magnetic flux. Magnetic reconnection at the magnetopause adds flux to the polar cap such that the dayside PCB moves to lower latitudes [*Siscoe and Huang*, 1985; *Milan and Slavin*, 2011]. Newly reconnected flux is then convected over the polar cap by the magnetosheath flow and into the magnetotail. Magnetic reconnection in the neutral sheet converts open magnetic flux from each pole into closed magnetic flux that eventually convects back toward the dayside magnetosphere. Observations of the time evolution of the PCB latitude can provide insight into the time history of both the dayside and nightside reconnection rates. This boundary can be identified in situ via the presence of solar wind-borne particle precipitation along the open field [*Winningham and Heikkila*, 1974; *Troshichev et al.*, 1996] or remotely from auroral emission observations [*Feldstein and Starkov*, 1967; *Eather and Akasofu*, 1969], though precipitation from trapped energetic particles in closed-field regions can obscure these observations.

At Earth, a large (~1000 times) increase in the magnetic field (**B**) magnitude from the magnetopause to the polar cap limits changes in polar cap latitude due to newly reconnected magnetic flux (≪1°/MWb). At Mercury, however, due to its comparatively weak internal magnetic field, a modest (~2–3 times) increase in the magnetic field strength from the magnetopause to the polar cap enables more measurable variations in the polar cap latitude (~10°/MWb). Furthermore, due to the absence of a stable radiation belt, Mercury's PCB can be identified clearly and unambiguously through in situ solar energetic particle (SEP) observations [*Gershman et al.*, 2015]. Mercury's polar cap therefore provides a highly sensitive laboratory for the study of small-scale variations in magnetic topology and reconnection rate.

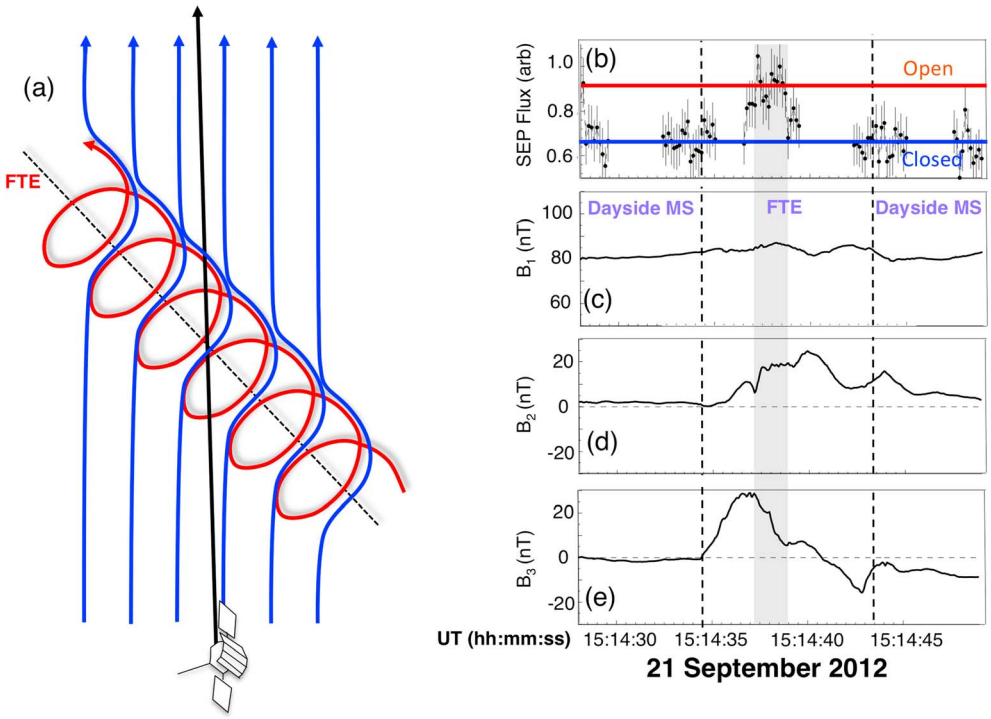

Figure 1. (a) Sketch of MESSENGER trajectory through an FTE observed on the dayside magnetosphere (LT 1500 h, Alt 1660 km) on 21 September 2012. A helical flux rope is embedded in Mercury's magnetospheric field. (b) Relative energetic particle flux as inferred by FIPS and magnetic field vectors from MAG in minimum variance coordinates with unit vectors in the (c) minimum variance direction: [−0.05, 0.20, 0.98], (d) intermediate variance direction: [−0.96, −0.29, 0.01], and (e) maximum variance direction: [0.29, −0.93, 0.20] in MSM coordinates with eigenvalues 1.8, 56.7, and 154.5, respectively. The FIPS-measured energetic particle rates are normalized by the average value in the dayside magnetosheath. Increased fluxes are observed inside the core of the FTE (shaded region) indicate that it transports open magnetic field. Gaps in the reported SEP flux indicate time periods between FIPS energy scans in which the sensor was not accumulating data.

Directly observed discrete units of reconnected flux on the dayside are associated with flux transfer events (FTEs), which are helical structures that carry magnetic flux [*Russell and Elphic*, 1979]. Individual FTEs carry ~1 MWb and up to ~0.1 MWb of magnetic flux at Earth and Mercury, respectively [*Slavin et al*. 2010a, 2012; *Imber et al*., 2014]. Because the average open magnetic flux content at Mercury is only ~2.5 MWb [*Johnson et al*., 2012], it has been suggested that showers of FTEs transport a significant portion of the open flux throughout the magnetosphere [*Slavin et al*. 2012; *Imber et al*. 2014]. However, no direct measurement of FTE topology that confirms their transport of open magnetic flux has yet been reported.

Here we examine high cadence (~150 ms) electron observations from the Fast Imaging Plasma Spectrometer (FIPS) [*Andrews et al*., 2007] and magnetic field from the Magnetometer experiment [*Anderson et al*., 2007] on the MErcury Surface, Space ENvironment, GEochemistry, and Ranging (MESSENGER) spacecraft from transits of the polar cap during strong SEP events. We provide the first direct measurement of the magnetic topology in an FTE at Mercury demonstrating that they can indeed be open, with one end connected to the planet and the other to the interplanetary magnetic field. In addition, we will use PCB fluctuations with respect to invariant latitude to infer the time history of the magnetopause reconnection electric field.

2. Data Selection and Processing

Nominally, FIPS samples ions with energy-per-charge (E/q) ratios between 10 eV/e and 13.3 keV/e in ~10 s using 60 logarithmically spaced steps [*Andrews et al*., 2007]. However, the thin (~1 mm) aluminum shielding and use of microchannel plate detectors for FIPS result in high sensitivity to the >1 MeV electrons and >10 MeV protons that bathe Mercury's magnetosphere during SEP events [*Gershman et al*., 2015]. Energetic protons have gyroradii that are large (e.g., ~1000 km) compared to Mercury's magnetospheric system (1 Mercury radius is ~2400 km). Consequently, they are not greatly deflected by the planetary magnetic

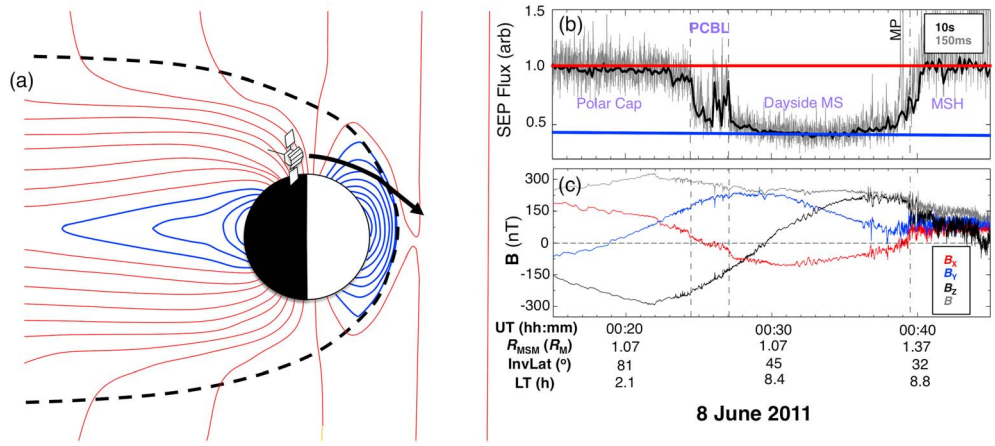

Figure 2. (a) Illustration of MESSENGER descending trajectory over Mercury's polar cap for a June 2011 SEP event. Open and closed magnetic field regions are indicated with red and blue lines, respectively. (b) Relative energetic particle flux as inferred by FIPS and (c) magnetic field vectors from MAG during 8 June 2011. The FIPS-measured energetic particle rates are normalized by the average value in the dayside magnetosheath. In the dayside closed-field region, fluxes drop significantly from their magnetosheath and polar cap levels. Fluctuations in SEP flux appear at ~00:26 UT with no corresponding large-amplitude fluctuations in the magnetic field data are labeled as the PCBL.

field, and their flux does not significantly decrease across the magnetopause. However, energetic electrons, particularly those precipitating over the polar cap, have much smaller gyroradii (~1–10 km), and consequently, we observe sharp changes in the FIPS energetic particle-induced count rates of its detectors that correspond with magnetospheric boundaries.

When the energetic electron rates from this event are high compared to nominal magnetospheric thermal plasma count rates, we can substantially increase measurement time resolution by using rates derived from the individual *E/q* channels instead of an average rate for each FIPS scan. Each ~10 s burst scan includes several seconds of high-voltage ramp-up such that there are small gaps between adjacent scans. Furthermore, although the timing within a scan is known to millisecond precision, due to truncation of the scan time in the spacecraft telemetry, there is an absolute uncertainty of the start of each scan by a fraction of a second. Finally, unphysical artifacts that arise from the FIPS processing of very high background signals manifest themselves as large, single *E/q* channel enhancements in the reported count rates. These electronic artifacts have been eliminated from the data set. Despite these caveats, we can effectively use FIPS' individual *E/q* channel rates to provide a ~150 ms proxy for changes in magnetic topology.

A close up of a magnetospheric FTE during an SEP event on 21 September 2012 demonstrates the ability of high-resolution FIPS measurements to reveal fine-scale magnetic topology in Figure 1. Magnetic field vectors for the duration of this FTE are shown in minimum variance coordinates [*Sonnerup and Cahill*, 1967; *Slavin et al*., 2010a], where the intermediate variance direction shows a relative core-field enhancement of ~20 nT and the maximum variance direction shows a corresponding bipolar signature indicative of helical structure embedded in the background magnetospheric field. A high average minimum variance component (~80 nT) indicates that MESSENGER merely clipped the edge of this structure. Nonetheless, increased SEP electron fluxes relative to the closed-field magnetosphere persist for approximately ~2 s that correspond with the observed center of the flux rope at 15:14:36 UT, indicating that its core transports open magnetic flux. Smaller-timescale (~0.5 s) fluctuations in electron fluxes may further indicate a complex magnetic topology, although such signatures are convolved with finite-gyroradii effects of the precipitating electrons.

FIPS energetic electron fluxes relative to magnetosheath levels are shown for an SEP event on 8 June 2011 in Figure 2. High energetic particle-induced count rates from both electrons and ions are observed as MESSENGER flies over the open-field polar cap region. The rates fluctuate near the PCB denoted as the polar cap boundary layer (PCBL) until reaching a steady value of ~0.5 throughout the dayside closed-field region, to which energetic electrons have limited access. After crossing the magnetopause (MP) at 00:39 UT into the dayside magnetosheath, the relative electron flux returns to ~1. In the PCBL, MESSENGER was approximately 1 Mercury radius (R_M) away from the Mercury-Solar-Magnetospheric (MSM) origin [*Anderson et al*., 2011], i.e.,

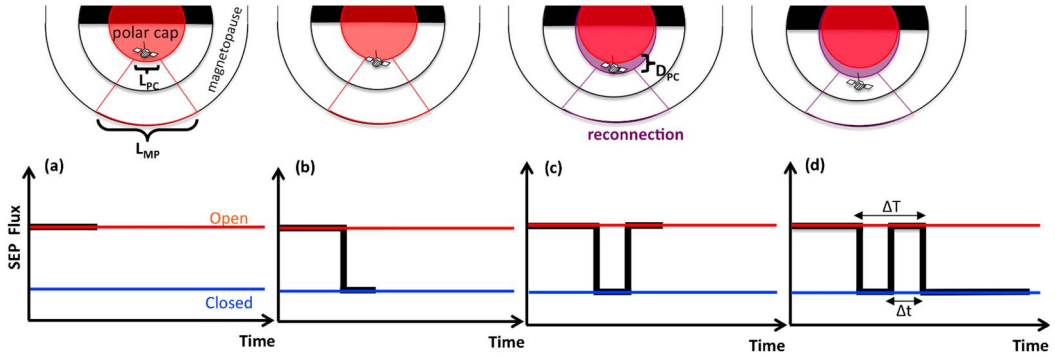

Figure 3. Top view illustration of MESSENGER trajectory over Mercury's polar cap. (a) While over the open-field region, FIPS measures high fluxes of energetic particles. (b) Fluxes drop sharply when the spacecraft enters the closed-field region. (c) If magnetic reconnection occurs at the magnetopause over length scale L_{MP}, the PCB expands by azimuthal length L_{PC} and polar length D_{PC}. If sufficient flux has reconnected to overtake the spacecraft, high SEP fluxes return until (d) the spacecraft once again exits the open-field region. Times between adjacent rises and falls of measured SEP flux provide information on the duration and strength of dayside magnetic reconnection.

on the sphere defining invariant latitude that is offset from the center of the planet by ~0.2 R_M. The PCBL is observed over an ~10° range of invariant latitudes corresponding to ~500 km in arc length on the sphere of 1 R_M. At the spacecraft location we further define a local spherical coordinate system where $\hat{\boldsymbol{r}}$ points radially outward from the MSM origin, $\hat{\boldsymbol{\theta}}$ points in the direction of decreasing invariant latitude, and $\hat{\boldsymbol{\phi}}$ completes the right-handed coordinate system and is oriented approximately duskward.

3. Analysis and Discussion

In a Dungey-like magnetospheric system, a newly reconnected parcel of plasma near the magnetopause becomes magnetically connected to a parcel of plasma at the PCB and flows over the polar cap with the magnetosheath flow. These parcels must remain magnetically connected until additional magnetic reconnection (e.g., in the magnetotail) reconfigures their magnetic topology. The PCBL is observed as MESSENGER alternatingly samples parcels of plasma that are magnetically connected and unconnected to the interplanetary magnetic field. Through field-aligned "Region 1" currents [*Anderson et al.*, 2014], the reconnection electric field in the diffusion region ($\mathbf{E_R} \approx E_R\,\hat{\boldsymbol{\phi}}$) maps to a dawn-dusk polar cap electric field ($\mathbf{E_{pc}} \approx E_{pc}\,\hat{\boldsymbol{\phi}}$) that drives antisunward plasma convection with velocity $\mathbf{v}_{pc} = (\mathbf{E_{pc}} \times \mathbf{B_{pc}})/B_{pc}^2$ [*Slavin et al.*, 2009]. Here in the northern hemisphere, the direction of Mercury's dipole, $\mathbf{B}_{pc}$ points planetward, i.e., in predominantly the $-\hat{\boldsymbol{r}}$ direction. Superimposed on this motion can be wave activity that creates localized variations in $\mathbf{v_{pc}}$, $\mathbf{E_{pc}}$, and $\mathbf{B_{pc}}$. We therefore consider the contributions of two effects to our observations: (1) back and forth wave motion of the PCB and (2) time-varying dayside magnetic reconnection. Magnetic reconnection in the magnetotail and the subsequent return of closed magnetic flux to the dayside will cause the PCB to contract and move poleward, resulting in an underestimation of reconnected flux. However, tail loading [e.g., *Slavin et al.*, 2010b] and return convection processes can act as low-pass filters for the circulation of magnetic flux in a magnetospheric system. Their effects, which are observed to have the timescale of 10^1–10^3 s, are not likely to be dominant on these very short (i.e., 10^0 s) timescales.

Steady antisunward motion of the magnetically connected magnetosheath and polar cap plasmas results in smooth poleward motion of the PCB with velocity $\mathbf{v}_{pc} = (\mathbf{E_{pc}} \times \mathbf{B_{pc}})/B_{pc}^2$ [*Dungey*, 1961]. Any disruption of this alignment due to PCB waves must produce a kink in the magnetic field, i.e., a change in B_θ/B. Because of the close (~1000 km) proximity of the magnetopause to the spacecraft and planetary core [*Anderson et al.*, 2014], kink angles of ±15° are required to reproduce apparent motions of the PCB plasmas per the ~500 km arc of invariant latitude transited by the spacecraft during these variations.

Alternatively, consider the illustration in Figure 3, which shows a top view of the magnetosphere. As MESSENGER descends out of the polar cap (Figure 3a), there is a sharp reduction in measured energetic electron flux. If dayside reconnection occurs (Figure 3b) over some azimuthal distance across the magnetopause, L_{MP}, a mapped distance in the polar cap, L_{PC}, will expand equatorward by a distance D_{PC} to accommodate

new open magnetic flux, i.e., $|\Phi| \approx |L_{PC} D_{PC} B_{PC}|$. If sufficient flux has been added to the polar cap, D_{PC} can grow large enough to overtake the spacecraft and open-field electron fluxes are measured. At a time ΔT later, MESSENGER then once again exits the polar cap region. The duration of observed increased electron flux is defined as Δt. We can therefore estimate the distance D_{PC} as

$$D_{PC} \approx R_M \Delta\theta_{sc} - \left(\boldsymbol{v}_{PC} \cdot \hat{\boldsymbol{\theta}}\right) \Delta t, \tag{1}$$

where $\Delta\theta_{sc}$ is the invariant latitude traversed by the spacecraft in time ΔT. Because the polar cap plasma velocity is in the $-\hat{\boldsymbol{\theta}}$ direction, the second term in equation (1) is positive. Therefore, antisunward convection increases our estimate of D_{PC}. This cycle of entering and exiting the polar cap can repeat multiple times provided that dayside reconnection continues with sufficient strength for the PCB to overtake the spacecraft (Figure 3c). Eventually, due to MESSENGER's orbital trajectory, the spacecraft will remain in the closed-field dayside magnetosphere until it crosses the dayside magnetopause (Figure 3d).

From Faraday's law of induction, the change of magnetic flux in the polar cap (Φ) due to dayside magnetic reconnection is equal to the integral of the electric field around the PCB, i.e., $\oint_{PC} \boldsymbol{E} \cdot d\boldsymbol{l} = -\frac{d\Phi}{dt}$. The right-hand side of this equation can be estimated as

$$-\frac{d\Phi}{dt} \approx -\frac{(\boldsymbol{B}_{PC} \cdot \hat{\boldsymbol{r}}) L_{PC} D_{PC}}{\Delta T}. \tag{2}$$

Here ΔT is used as the time over which flux was added to the polar cap. ΔT is an upper bound for the true time, which cannot be evaluated due to observations from a single spacecraft. Because Mercury's magnetic field is predominantly in the $-\hat{\boldsymbol{r}}$ direction over the northern polar cap, $\frac{d\Phi}{dt} < 0$.

The largest contribution to the integral around the PCB is the dawn-dusk electric field $\mathbf{E}_{PC}$ along distance L_{PC} such that

$$\oint \boldsymbol{E} \cdot d\boldsymbol{l} \approx E_{PC} L_{PC}. \tag{3}$$

For the case that the PCB velocity is dominated by $\mathbf{E} \times \mathbf{B}$ drift,

$$-\left(\boldsymbol{v}_{PC} \cdot \hat{\boldsymbol{\theta}}\right) \approx E_{PC} |\boldsymbol{B}_{PC} \cdot \hat{\boldsymbol{r}}| / B_{PC}^2. \tag{4}$$

We can then combine equations (1)–(4) to solve for the magnitude of the polar cap electric field,

$$E_{PC} \approx \frac{B_{PC}^2}{|\boldsymbol{B}_{PC} \cdot \hat{\boldsymbol{r}}|} \frac{\Delta\theta_{sc}}{\Delta T - \Delta t}. \tag{5}$$

Finally, because the PCB electric field maps directly to magnetopause diffusion region as $E_{PC} L_{PC} \approx E_R L_{MP}$ [e.g., *Toffoletto and Hill*, 1989], we can express the reconnection electric field as a function of measurements over the polar cap,

$$E_R \approx \frac{B_{PC}^2}{|\boldsymbol{B}_{PC} \cdot \hat{\boldsymbol{r}}|} \frac{R_M \Delta\theta_{sc}}{\Delta T - \Delta t} \left(\frac{L_{PC}}{L_{MP}}\right). \tag{6}$$

For a PCB latitude of ~60° and a magnetopause standoff distance of ~1.5 R_M, we use $L_{PC}/L_{MP} \sim 1/3$. This value assumes that the azimuthal extent of the dayside reconnection along a sphere representing the magnetopause is approximately equal to the extent of the PCB.

The time history of relative energetic electron flux, B_θ/B, and the reconnection electric field calculated from equation (6) are shown in Figure 4 for two successive crossings of Mercury's PCBL during the June 2011 SEP event. Changes in the magnetic field direction (B_θ/B) are small (<5°) and are largely uncorrelated with the ~5 s variation in energetic electron fluxes. We conclude that the observed PCBL signatures are not the result of PCB waves but rather correspond to time changes in the rate of magnetic reconnection as illustrated in Figure 3. The mean and standard deviation of Δt and ΔT calculated from the set of observed fluctuations are 6.7 ± 2.7 s and 8.8 ± 3.4 s, respectively. These times result in derived reconnection electric fields that range from $E_R \sim 0.3$–3 mV/m.

A solar wind speed of ~300 km/s was estimated from FIPS data using adjacent orbits where the plasma peak energy could be observed over the energetic particle fluxes [*Gershman et al.*, 2012]. This speed combined

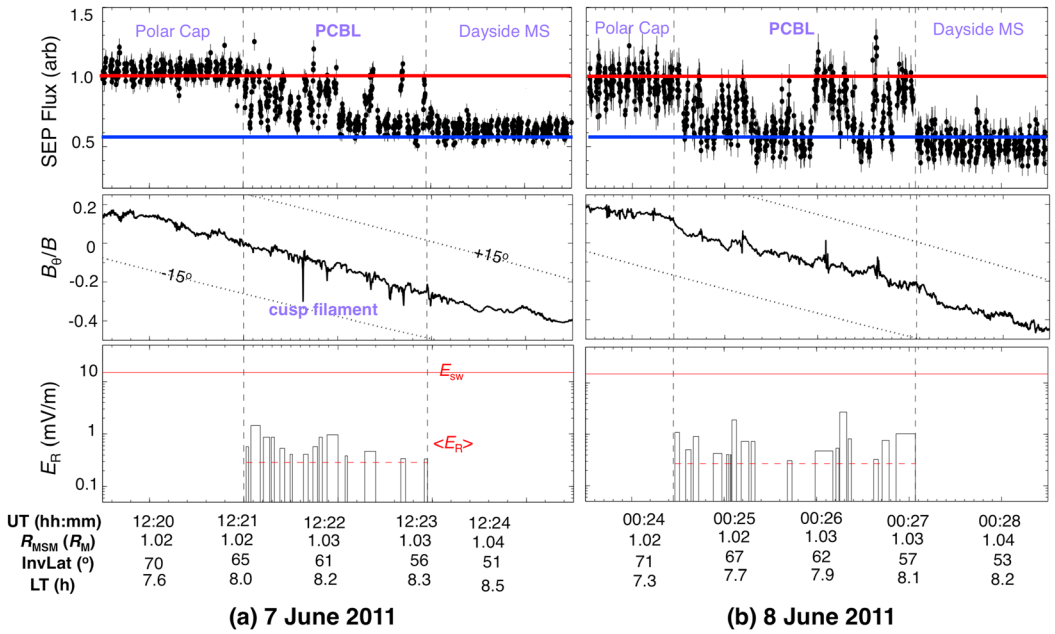

Figure 4. PCBL transits of MESSENGER for two successive orbits on (a) 7 June 2011 and (b) 8 June 2011. The top panels show high cadence (~150 ms) energetic particle fluxes from FIPS normalized to their magnetosheath (MSH) values. Using the timing of the observed bursts in SEP flux, the reconnection electric field at the magnetopause is estimated in the bottom panels. Bursts of ~0.3–3 mV/m fields correspond to peak and average reconnection rates of ~0.2 and 0.02, respectively.

with an IMF strength of ~50 nT observed outside of the bow shock results in an estimated solar wind electric field (E_{SW}) of ~15 mV/m. The derived maximum instantaneous and average relative reconnection rates (E_R/E_{SW}) are therefore ~0.2 and ~0.02, respectively. Because the spacecraft is a single-point measurement, the true reconnection rate for these intervals is likely between our reported average and instantaneous rates. Nonetheless, the apparent reconnection rate varies on the order of the ion gyroperiod at the magnetopause, i.e., a few seconds. Such modulations are consistent with particle-in-cell simulations of both symmetric and asymmetric magnetic reconnection, where small-scale structure and secondary islands can temporarily disrupt or enhance the rate of reconnection [*Daughton et al.*, 2006; *Karimabadi et al.*, 2007].

Dayside FTEs have been observed at Mercury with similar timescales as these PCBL fluctuations, and some flux-rope-like structures are observed near the magnetopause for these orbits. We also observe a cusp filament in Figure 4a at 12:21:30 UT, a magnetic structure of diamagnetic origin, whose presence has been previously correlated with high FTE activity; it was proposed that these cusp filaments are the polar cap foot points of FTEs in the dayside magnetopause [*Slavin et al.*, 2014; G. Poh et al., MESSENGER Observations of Cusp Plasma Filaments at Mercury, submitted to *Journal of Geophysical Research: Space Physics*, 2016]. Our determination of the open-closed boundary is independent of the magnetic field measurements such that we do not expect to find a one-to-one correspondence of cusp filaments for each PCBL structure. Our observations suggest that the contribution of bursty dayside reconnection at Mercury is likely underestimated for any given MESSENGER polar cap transit when using magnetic field signatures alone. Based on the duration of observed events and their **E × B** drift velocities, we estimate a latitudinal spatial extent ranging from 25 km to 100 km. These spatial scales mapped to the MP correspond to ion inertial scale lengths in Mercury's magnetic diffusion region.

Circular magnetic foot points for these structures at the sampled altitudes would encompass magnetic fluxes of ~10^{-3} MWb. This flux is an order of magnitude smaller than previous estimates of the flux carried by a single FTE [*Imber et al.*, 2014]. Because the measured PCBL fluctuations provide constraints on latitudinal extent of these structures, this discrepancy suggests that either the foot point of an FTE in the polar cap is elongated in local time or a complex open-closed topological structure exists inside each flux rope such that multiple observed PCBL events map to a single FTE. In two-dimensional reconnection, there is a clearly defined separatrix that prohibits the formation of such topology. However, fully three-dimensional simulations can

produce complex topological domains at the smallest ion spatial scales [*Dorelli and Bhattacharjee*, 2009]. Some variability in energetic particle fluxes inside the FTE shown in Figure 1 suggests that such fine-scale features could be present. Regardless of the PCBL structure being spatial or temporal in nature, we are probing the smallest ion scales relevant to reconnection physics at Mercury.

4. Concluding Remarks

Mercury's small magnetosphere is a sensitive magnetic reconnection laboratory. Energetic electrons observed by FIPS on MESSENGER during SEP events provide valuable field line tracers that map Mercury's magnetospheric topology at high cadence. Enhanced SEP fluxes observed within an FTE provide confirmation that such structures are a mechanism of open-flux transport at Mercury. In addition, quick changes in magnetic topology were observed near the PCB for two successive orbits that correspond to ion kinetic scales and may provide a proxy for the time history of magnetic reconnection at the magnetopause. Such temporal variations are not easily determined at Earth as measurements from spacecraft constellations (e.g., Magnetospheric Multiscale) can only reconstruct the properties of the magnetic diffusion region in a single instant rather than provide a time history of reconnection rate. Our analysis suggests that magnetic reconnection at Mercury may be a fundamentally bursty process, where strong modulations of the reconnection rate occur at ion gyroperiod scales.

Acknowledgments

The authors wish to acknowledge the MESSENGER team, in particular the FIPS and MAG instrument teams, for their efforts in producing fields and particle data at Mercury. MESSENGER data used in this study are available from the Planetary Data System (http://pds.nasa.gov). Uncorrected FIPS data (ESS-E/V/H/SW-EPPS-2-FIPS-RAWDATA-V2.0) were used to estimate relative energetic particle fluxes. G.A.D. is supported by a NASA Postdoctoral Program appointment at the NASA Goddard Space Flight Center, administered by Oak Ridge Associated Universities through a contract with NASA. This work was also supported by the NASA Discovery Data Analysis Program under grant NNX15AK88G.

References

Anderson, B. J., M. H. Acuña, D. A. Lohr, J. Scheifele, A. Raval, and H. Korth (2007), The Magnetometer instrument on MESSENGER, *Space Sci. Rev.*, *131*, 417–450, doi:10.1007/s11214-007-9246-7.

Anderson, B. J., C. L. Johnson, H. Korth, M. E. Purucker, R. M. Winslow, J. A. Slavin, S. C. Solomon, R. L. McNutt Jr., J. M. Raines, and T. H. Zurbuchen (2011), The global magnetic field of Mercury from MESSENGER orbital observations, *Science*, *333*, 1859–1862, doi:10.1126/science.1211001.

Anderson, B. J., C. L. Johnson, H. Korth, J. A. Slavin, R. M. Winslow, R. J. Phillips, R. L. McNutt Jr., and S. C. Solomon (2014), Steady-state field-aligned currents at Mercury, *Geophys. Res. Lett.*, *41*, 7444–7452, doi:10.1002/2014GL061677.

Andrews, G. B., et al. (2007), The Energetic Particle and Plasma Spectrometer instrument on the MESSENGER spacecraft, *Space Sci. Rev.*, *131*, 523–556.

Daughton, W., J. Scudder, and H. Karimabadi (2006), Fully kinetic simulations of undriven magnetic reconnection with open boundary conditions, *Phys. Plasmas*, *13*, 072101-1–072101-15, doi:10.1063/1.2218817.

Dorelli, J. C., and A. Bhattacharjee (2009), On the generation and topology of flux transfer events, *J. Geophys. Res.*, *114*, A06213, doi:10.1029/2008JA013410.

Dungey, J. W. (1961), Interplanetary magnetic fields and the auroral zone, *Phys. Rev. Lett.*, *6*, 47.

Eather, R. H., and S.-I. Akasofu (1969), Characteristics of polar cap auroras, *J. Geophys. Res.*, *74*, 4794–4798, doi:10.1029/JA074i019p04794.

Feldstein, Y. I., and G. V. Starkov (1967), Dynamics of auroral belt and polar geomagnetic disturbances, *Planet. Space Sci.*, *15*, 209.

Gershman, D. J., T. H. Zurbuchen, L. A. Fisk, J. A. Gilbert, J. M. Raines, B. J. Anderson, C. W. Smith, H. Korth, and S. C. Solomon (2012), Solar wind alpha particles and heavy ions in the inner heliosphere observed with MESSENGER, *J. Geophys. Res.*, *117*, A00M02, doi:10.1029/2012JA017829.

Gershman, D. J., et al. (2015), MESSENGER observations of solar energetic electrons within Mercury's magnetosphere, *J. Geophys. Res. Space Physics*, *120*, 8559–8571, doi:10.1002/2015JA021610.

Imber, S. M., J. A. Slavin, S. A. Boardsen, B. J. Anderson, H. Korth, R. L. McNutt Jr., and S. C. Solomon (2014), MESSENGER observations of large dayside flux transfer events: Do they drive Mercury's substorm cycle? *J. Geophys. Res. Space Physics*, *119*, 5613–5623, doi:10.1002/2014JA019884.

Johnson, C. L., et al. (2012), MESSENGER observations of Mercury's magnetic field structure, *J. Geophys. Res.*, *117*, E00L14, doi:10.1029/2012JE004217.

Karimabadi, H., W. Daughton, and J. Scudder (2007), Multi-scale structure of the electron diffusion region, *Geophys. Res. Lett.*, *34*, L13104, doi:10.1029/2007GL030306.

Milan, S. E., and J. A. Slavin (2011), An assessment of the length of variability of Mercury's magnetotail, *Planet. Space Sci.*, *59*, 2058–2065, doi:10.1016/j.pss.2011.05.007.

Parker, E. N. (1957), Sweet's mechanism for merging magnetic fields in conducting fluids, *J. Geophys. Res.*, *62*, 509–520, doi:10.1029/JZ062i004p00509.

Russell, C. T., and R. C. Elphic (1979), ISEE observations of flux transfer events at the dayside magnetopause, *Geophys. Res. Lett.*, *6*, 33–36, doi:10.1029/GL006i001p00033.

Siscoe, G. L., and T. S. Huang (1985), Polar cap inflation and deflation, *J. Geophys. Res.*, *90*, 543–547, doi:10.1029/JA090iA01p00543.

Slavin, J. A., et al. (2009), MESSENGER observations of magnetic reconnection in Mercury's magnetosphere, *Science*, *324*, 606–610, doi:10.1126/science.1172011.

Slavin, J. A., et al. (2010a), MESSENGER observations of large flux transfer events at Mercury, *Geophys. Res. Lett.*, *37*, L02105, doi:10.1029/2009GL041485.

Slavin, J. A., et al. (2010b), MESSENGER observations of extreme loading and unloading of Mercury's magnetic tail, *Science*, *329*, 665–668, doi:10.1126/science.1188067.

Slavin, J. A., et al. (2012), MESSENGER observations of a flux-transfer-event shower at Mercury, *J. Geophys. Res.*, *117*, A00M06, doi:10.1029/2012JA017926.

Slavin, J. A., et al. (2014), MESSENGER observations of Mercury's dayside magnetosphere under extreme solar wind conditions, *J. Geophys. Res. Space Physics*, *119*, 8087–8116, doi:10.1002/2014JA020319.

Sonnerup, B. U., and L. J. Cahill Jr. (1967), Magnetopause structure and attitude from Explorer 12 observations, *J. Geophys. Res.*, *72*, 171–183, doi:10.1029/JZ072i001p00171.

Sweet, P. A. (1958), The neutral point theory of solar flares, in *Electromagnetic Phenomena in Cosmical Physics*, edited by B. Lehnert, pp. 123–134, Cambridge Univ. Press, London.

Toffoletto, F. R., and T. W. Hill (1989), Mapping of the solar wind electric field to the Earth's polar caps, *J. Geophys. Res.*, *94*, 329–347, doi:10.1029/JA094iA01p00329.

Troshichev, O. A., E. M. Shishkina, C.-I. Meng, and P. T. Newell (1996), Identification of the poleward boundary of the auroral oval using characteristics of ion precipitation, *J. Geophys. Res.*, *101*, 5035–5046, doi:10.1029/95JA03634.

Winningham, J. D., and W. J. Heikkila (1974), Polar cap auroral electron fluxes observed with Isis 1, *J. Geophys. Res.*, *79*, 949–957, doi:10.1029/JA079i007p00949.